Trop J Nat Prod Res, November 2020; 4(11):945-952 **ISSN 2616-0684 (Print)**
ISSN 2616-0692 (Electronic)

Tropical Journal of Natural Product Research

Available online at https://www.tjnpr.org

Original Research Article

Nanoencapsulation of *Syzygium polycephalum* Extract Using Folate Modified κ-Carrageenan as Vehicles for Pronounced Anticancer Activity

Andika P. Wardana[1], Nanik S. Aminah[1,2]*, Mochamad Z. Fahmi[1], Alfinda N. Kristanti[1,2], Haninda I. Zahrah[3], Yoshiaki Takaya[4], M. Iqbal Choudhary[5]

[1]*Department of Chemistry, Faculty of Science and Technology, Universitas Airlangga, Kampus C-UNAIR, Jl. Mulyorejo, Surabaya 60115, Surabaya, Indonesia*
[2]*Biotechnology of Tropical Medicinal Plants Research Group, Universitas Airlangga, Surabaya 60115, Surabaya, Indonesia*
[3]*Faculty of Dental Medicine, Universitas Airlangga, Kampus A-UNAIR, Jl. Mayjen Prof. Dr. Moestopo 47, Surabaya 60131, Surabaya, Indonesia*
[4]*Department of Pharmacy, Meijo University, Nagoya, Japan*
[5]*H. E. J. Research Institute of Chemistry, International Center for Chemical and Biological Sciences, University of Karachi, Karachi-75270, Pakistan*

ARTICLE INFO

Article history:
Received 01 October 2020
Revised 28 October 2020
Accepted 27 November 2020
Published online 30 November 2020

ABSTRACT

S. polycephalum (*Sp*) is an important species of the genus Syzygium. 3,4,3'-tri-O-methyl ellagic acid obtained from *Sp*, has potential as a natural anticancer agent. The drawback of natural products as medicine is their non-specific effects and poor solubility, so a better drug delivery system is needed to overcome this challenge. This study utilizes κ-carrageenan and carrageenan folate (Cf) as the carrier matrix. Sp-CNPs and Sp-CfNPs can increase the anticancer activity of *Sp* extract. The addition of folate groups to carrageenan gave better results in delivering the *Sp* extract drug on the HeLa cell line and T47D cell line. The free *Sp* extract was able to inhibit the growth of HeLa cancer cells with EC_{50} 114.19 ± 10.31 µg/mL, while both *Sp*-CNPS and *Sp*-CfNPs nanocapsules showed EC_{50} 79.19 ± 13.96 µg/mL and EC_{50} 48.77 ± 15.91 µg/mL. In T47D cells, the free *Sp* extract showed EC_{50} 498.33 ± 110.72 µg/mL. *Sp*-CNP nanocapsules were able to increase the anticancer activity of free Sp extract with EC_{50} 80.62 ± 12.59 µg/mL, whereas *Sp*-CfNP performed anticancer activity against T47D cells with EC_{50} 48.52 ± 2.76 µg/mL.

***Keywords*:** Anticancer, Drug delivery system, Folate receptor, Nanoencapsulation, *Syzygium polycephalum*.

Introduction

Cancer is among the leading causes of death worldwide. The prevalence of cancer is expected to increase rapidly with population growth, ageing, and changing lifestyles.[1] Based on 2018 GLOBOCAN data, there are around 18.1 million new cancer cases and 9.6 million deaths due to cancers. In the same year, breast cancer was ranked as the second deadliest disease after lung cancer, with 2.088.849 new cases and 626.679 deaths. Cervical cancer is also one of the leading causes of cancer-related deaths after breast cancer. There were 569.847 new cases and 311.365 deaths from cervical cancer.[2] So far, Cancer treatment mainly involves chemotherapy, radiotherapy, and surgery. Some of the most commonly used chemotherapy drugs are anti-proliferative compounds, DNA intercalating agents, anti-tubulins, hormones, and targeted molecular therapy.[3] The use of chemotherapy drugs can cause adverse effects, such as hair loss, bone marrow suppression, drug resistance, gastrointestinal lesions, neurological dysfunction, and cardiac toxicity.[4] This has led to a renewed interest in developing safe and effective natural ingredient-based anti-cancer medicines.[5]

Folate receptors (FR) are attractive cancer targets because of overexpression in various types of cancer.[6] This expression can be useful in targeting therapeutic compounds directly on cancer cells using many avenues[7] Targeting cancer drugs through conjugation of specific ligands with the number of nanodrugs encapsulated is very promising in the drug delivery system.[8] Folic acid is a ligand that provides diagnostic and therapeutic content in cancer imaging and therapy that express FR.[9] The advantages of folic acid are small molecular size (441 Da), stable at wide temperature and pH changes, inexpensive, non-immunogenic. They can maintain the binding of FR after conjugation with drugs or diagnostic markers.[10]

Previous studies have revealed that several species of the genus *Syzygium* have the anticancer potential. These include *S. cumini*,[11] *S. aromatic*,[12] *S. campanulatum*,[13] *S. samarangense*,[14] *S. caryophyllatum*,[15] *S. benthamianum*,[16] *S. fruticosum*,[17] and *S. alternifolium*.[18] *S. polycephalum* contains ellagic acid derivatives, such as 3,4,3'-tri-*O*-methyl ellagic acid.[19] Ellagic acid and its derivatives have been reported for their anticancer activity. Ellagic acid derivatives are reported to inhibit breast cancer cells,[20] osteogenic sarcoma,[21] pancreatic cancer,[22] ovarian cancer,[23] nasopharyngeal carcinoma,[24] lymphoma,[25] prostate cancer, [26] colorectal cancer,[27] and oral cancers.[28] Ellagic acid derivatives, such as 3,3'-di-*O*-methyl ellagic acid-4'-*O*-*β*-d-xylopyranoside from *Euphorbia hylonoma* can inhibit the growth of HepG2 cancer cells.[29] 4,4'-Di-*O*-methyl ellagic acid derivatives can inhibit the development of colon cancer cells. [30] Ellagic acid nanoencapsulation can increase the solubility and antioxidant activity.[31] Besides, nano ellagic acid can reduce the nephrotoxicity and hepatotoxic effects of cisplatin.[32,33] Nanoencapsulation pomegranate can improve the chemoprevention of breast cancer cells (MCF-7).[34]

Natural products often exhibit good activity *in vitro*, but may not show satisfactory results *in vivo* due to non-specificity, and poor solubility.[35] One approach to overcome these weaknesses is to use novel drug delivery systems (NDDS), increasing the therapeutic effect, and reducing toxicity. The nanotechnology approach has been applied to cancer chemotherapy to reduce toxicity and increase stability,

*Corresponding author. E mail: nanik-s-a@fst.unair.ac.id
Tel: +62-31-5936501 Fax: +62-31-5936502

Citation: Wardana AP, Aminah NS, Fahmi MZ, Kristanti AN, Zahrah HI, Takaya Y, and Choudhary MI. Nanoencapsulation of *Syzygium polycephalum* Extract Using Folate Modified κ-Carrageenan as Vehicles for Pronounced Anticancer Activity. Trop J Nat Prod Res. 2020; 4(11):945-952. doi.org/10.26538/tjnpr/v4i11.17

Official Journal of Natural Product Research Group, Faculty of Pharmacy, University of Benin, Benin City, Nigeria

bioavailability, and selectivity. [36] Nanoencapsulation is an application of nanotechnology that can improve stability, and bioavailability of bioactive compounds because nano-size can increase the surface area.[37] This research focuses on the use of κ-carrageenan, and conjugated carbohydrate folic acid, as NDDS for *S. polycepahum* nanoencapsulation. The use of carrageenan folate as a carrier for *S. polycepahum* bioactive compound targets folate receptors on cancer cells. The study conducted was the elucidation of bioactive compounds from *S. polycephalum*. The characterization of nanocapsules includes physicochemical properties, stability, loading, release and anticancer activity *in vitro* on HeLa cell line and T47D cell line.

Materials and Methods

Materials

4-Dimethylaminopyridine (DMAP) (Sigma-Aldrich); *N*-(3-dimethylaminopropyl)-*N*'-ethylcarbodiimide hydrochloride (EDCl) (Sigma-Aldrich); distilled water; folic acid; dimethyl sulfoxide (DMSO); phosphate buffer pH 4, pH 7, pH 9; doxorubicin; κ-carrageenan; 3-(4,5'-dimethylthiazol-2-yl)-2,5-diphenyltetrazolium (MTT); phosphate buffer saline (PBS), HCl, sodium dodecyl sulfate (SDS); methanol; *n*-hexane; dichloromethane (DCM); silica gel 60 (0.063-0.200 mm) (Merck); and TLC silica gel 60 F254 (Merck). All chemical are used directly without any particular purification.

Extraction and Isolation

S. polycephalum bark was obtained in March 2020 from Mount Lawu, Ngawi, East Java, Indonesia at an altitude of 917 meters above sea level with coordinates 7° 33'19.8 "S 111° 13'06.0" E. *S. polycephalum* bark powder (3 kg) was macerated with 6 L methanol for 24 hours at room temperature. The filtrate was passed through a Buchner funnel to obtain methanol extract. The extract of *S. polycephalum* was then concentrated on a rotary vacuum evaporator to obtain a thick methanol extract (164 g). The methanol extract was further partitioned with *n*-hexane, and DCM. A total of 15 g of n-hexane and 6.7 g of DCM extract were obtained. Two (2) g of DCM extract (Sp extract) was fractionated by column chromatography with *n*-hexane: DCM: methanol. The resulting fractions were monitored with TLC. The fractions were then analyzed by UV-Vis (Shimadzu UV-1800), FTIR (Shimadzu IRTracer-100), DART-MS (Thermo Scientific Inc.), ^{1}H-NMR (Bruker AV NEO 500 MHz), and ^{13}C-NMR (Bruker Avance NEO 600 MHz LC Cryoprobe) for secondary metabolites.

Synthesis of carrageenan folate (Cf)

Carrageenan folate was synthesized by reacting folic acid with κ-carrageenan. The first stage involved folic acid that was reacted with EDCl. In the second stage, κ-carrageenan was reacted with DMAP. Both mixtures from the first and second stages were reacted. Finally, the products were characterized using UV-Vis spectrometer, FTIR, and TGA (Perkin Elmer, TGA 4000).

Synthesis of Sp-CNPs and Sp-CfNPs

Sp extract was dissolved in DMSO and added to κ-carrageenan in a ratio of 1/4. The mixture was then treated with an ultrasonic probe (JY-9211DN, Ningbo Scientz Biotechnology, China) to form *Sp*-CNPs. The same process was used for the synthesis of *Sp*-CfNPs, which replaced κ-carrageenan with carrageenan folate.

Characterization and stability Sp-CNPs and Sp-CfNPs

The physicochemical properties of *Sp*-CNPs, and *Sp*-CfNPs were measured using a polydispersity index (PDI), zeta potential (ζ), and particle size (Dynamic Light Scattering, Zetasizer Nano ZS, Malvern). FTIR was used for the analysis of the functional groups of NPs produced. The powdered nanocapsules were obtained by freeze drying **(**Alpha 1-2 LDplus, CHRIST) from the colloidal solution. The morphology of the freeze-dried NPs was characterized by TEM (JEOL JEM 1400). This method's protocol was done by re-dissolved in ethanol, drop it on the copper grid (300 mesh x 250 µm), and put it on the TEM instrument after the drying process. TGA (Perkin Elmer TGA 4000) was also used to determine the decomposition of NPs. Further stability of *Sp*-CNPs, and *Sp*-CfNPs was tested for parameters, such as pH, temperature, and salt, the changes in the UV-Vis absorption bands at 200 nm – 500 nm, and the degree of turbidity of nanoparticles.

Loading and release of Sp-CNPs and Sp-CfNPs

The calculation of Loading Efficiency (LE) and Loading Amount (LA) was calculated, as shown in equations (1) and (2), respectively.

$$\%\text{LE} = \frac{\text{mass of Sp extract on NPs}}{\text{mass of Sp extract in feed}} \text{ x } 100\% \quad \ldots(1)$$

$$\%\text{LA} = \frac{\text{mass of Sp extract on NPs}}{\text{mass of NPs}} \text{ x } 100\% \quad \ldots(2)$$

Release tests of *Sp*-CNPs and *Sp*-CfNPs were carried out through a dialysis process using a semipermeable cellulose membrane with PBS (pH 4, 7, and 9) as an outer membrane solution. The release was observed for 24 h by sampling 1 mL aliquots at a time with periodic interval. The concentration of the active compound in *Sp* extract (3,4,3'-tri-*O*-methyl ellagic acid released was determined based on absorbance and corrected by equation (3): [38]

$$Ct' = Ct + \frac{v}{V}\sum_{0}^{i-t} Ct \quad \ldots(3)$$

Where Ct '= correction concentration at time t
Ct = measured concentration at time t
v = volume of aliquots
V = total PBS volume

Cytotoxicity assessment

HeLa and T47D cancer cells with 80% confluent conditions were grown in 96-well plates and incubated for 24 h with 5% CO_2 flow at 37^{o}C. Next, the cell media was removed. Each well was filled with samples of *Sp*-CNPs, and *Sp*-CfNPs with a certain concentration. The cells were re-incubated for 24 h, and then 10 µL of MTT (5 mg / mL) was added. After adding MTT cells, they were incubated for 4 h, and 10% SDS in 0.01 N HCl was added to a final volume of 100 µL. The absorbance was calculated with ELISA reader at λ_{max} 550 nm. Based on the absorbance, the viability of cells (Hella, and T47D) were calculated as:

$$\text{Cell viability (\%)} = \frac{\text{A}_{\text{sample}} - \text{A}_{\text{blank}}}{\text{A}_{\text{control}} - \text{A}_{\text{blank}}} \text{ x } 100\% \quad \ldots(4)$$

EC_{50} ± SE (standard error) calculations are determined using response dose analysis or sigmoidal fitting using the Origin® 2018 application.

Statistical analysis

Data was repeated three times (n = 3) and analyzed by one-way ANOVA to determine the effect of anticancer activity of *Sp* extract encapsulated with κ-carrageenan and carrageenan folate. If the value of $p < 0.05$, it shows a statistically significant difference.

Results and Discussion

Elucidation of structure

The column chromatography of *S. polycephalum* yielded 4 main fractions, namely fraction 1 (1-3), 2 (4-7), 3 (8-20), and 4 (21-42). Fraction 2 (13.4 mg), based on TLC profiles, had the target compound, ellagic acid derivatives compound with Rf 0.35. It had a characteristic yellowish-white powder, m.p. 268-269^{o}C. The UV-Vis spectrum (MeOH, λ_{max}) of the isolate had a maximum absorbance at 247.7 (benzene group), and 372.2 nm (carbonyl group) (Supplementary Fig S1). FTIR absorbance (KBr, λ_{max}) of the isolated compound was at 3421 (OH stretch), 2945, 2918, 2850 (CH stretch),

1751, 1728 (C = O stretch), 1608, 1577, 1492 (C-C benzene ring system), 1363 (CH_3 group), 1244, 1118, and 1091 cm^{-1} (-O-aryl, and -OCH_3) (Supplementary Fig S2). The molecular formula $C_{17}H_{12}O_8$ was deduced from the DART-MS (*m/z* 345.0609 [M + H^+]) (Supplementary Fig S3). Based on the ^{1}H-NMR spectrum (Table 1), 2 aromatic ring resonances were found in the ellagic acid skeleton at δ_H 7.63 (1H, s, H-5), and 7.52 (1H, s, H-5'). The signal at three methoxy groups showed three proton singlets at δ_H 4.04, 4.03, and 3.99 (3H, s, -OCH_3). The signal at δ_H 10.84 (1H, *br*) indicated a hydroxy group on the aromatic ring (Supplementary Fig S4). There were 17 carbon signals in the^{13}C-NMR spectrum. Signals at δ_C 141.5 (C, C-2), and 140.9 (C, C-2') were due to the benzene carbons bonded to a lactone group. The signals at δ_C 107.5 (C, C-5), and 111.7 (C, C-5') were for the aromatic CH, whereas signals at δ_C 112.0 (C, C-1), and 111.1 (C, C-1') were assigned to aromatic carbons. The other two signals at δ_C 140.9 (C, C-3), and 140.3 (C, C-3') was for the benzene carbons with the methoxy group. The signals at δ_C 152.8 (C, C-4), and 153.8 (C, C-4') were due to aromatic carbons, substituted with methoxy, and hydroxy groups, respectively. The three signals at δ_C 61.3 (-OCH_3, C-3), 61.0 (-OCH_3, C-3'), and 56.7 (-OCH_3, C-4) were due to the ~~OCH_3~~ methoxy group (Supplementary Fig S5). The ^{1}H and ^{13}C-NMR chemical shift values of the isolates and reference[39] are shown in Table 1. Based on the interpretation of UV-Vis, FTIR, ~~FTMS~~ DART-MS, ^{1}H-NMR, ^{13}C-NMR, HSQC, and HMBC data, the structure of the compounds isolated from *S. polycephalum* was deduced as 3,4,3'-tri-*O*-methyl ellagic acid (Figure 1).

Cf Characterization

Esterification of κ-carrageenan with folic acid in carrageenan folate catalyzed was resulted by EDCl and DMAP. Folic acid will react with EDCl that activate the carboxyl group in folic acid and release the proton release, form folic anion and protonated EDCl. Folic anion will attack the carbodiimide EDCl to form O-acylisourea compound which will react with DMAP as a nucleophile. It is stronger than the alcohol group to produce ester intermediates that are very reactive to the -OH group of κ-carrageenan to produce an ester, namely carrageenan folate.[40] (Supplementary Figure S6)

The characterization of κ-carrageenan, and carrageenan folate using a UV-Vis spectrometer is presented in Figure 2. κ-Carrageenan is a straight-chain polysaccharide with a disaccharide repeat unit consisting of (1,3)-β-galactose-4-sulfate and (1,4)-α-3,6-anhydro-galactose residues (Figure 3).[41]

κ-Carrageenan is formed from its precursor μ-carrageenan. μ-Carrageenan is composed of D-galactose-4-sulfate, and D-galactose-6-sulfate monomers. κ-Carrageenan shows terminal absorption at $\lambda_{max} \leq$ 200 nm in the UV spectrum, as it does not have a chromophore or an auxochrome group. Folic acid uptake by UV-Vis spectrometer showed two absorption bands at 280.5, and 353 nm. The transition of $n \rightarrow \pi^*$ occurred at 280 nm, while $\pi \rightarrow \pi^*$ transition occurred at 353 nm. Compounds resulting from the synthesis of κ-carrageenan esterification with folic acid showed an absorption band at 280 nm due to $n \rightarrow \pi^*$ transition in folic acid. This indicated the formation of carrageenan folate. κ-Carrageenan was analyzed from the FTIR spectrum. Several functional groups in the structure showed absorptions. It has been explained previously that κ-carrageenan is composed of D-galactose-4-sulfate with α bonds at positions 1 and 3, and 3,6-anhydro-D-galactose with β bonds at positions 1 and 4. The typical wave number of D-galactose-4-sulfate was is in the region of 840 - 850 cm^{-1}, while the absorption of 3,6-anhydro-D-galactose between 925 - 935 cm^{-1} (Figure 4).[42] However, κ-Carrageenan, Cf, and folic acid cannot be distinguished from the FTIR spectrum because all three compounds have functional groups that appear at the same wavenumbers.

The thermogravimetric technique was then used to determine the mass of a component as a function of temperature. This was used to determine the composition and interaction in a component. TGA results are shown in Figure 5A, while the first derivative function is shown in Figure 5B. κ-Carrageenan has 3 times of decomposition, Cf has 4 times of decay, and folic acid has two decomposition times. Cf shows an additional peak at 127 ^oC, which indicates the bending between κ-carrageenan and folic acid. Besides this, Cf's peak intensity at 202 ^oC and 298 ^oC was characteristic of the κ-carrageenan. Based on this data, Cf seems to have been successfully synthesized from κ-carrageenan, and folic acid.

Sp-CNPs and Sp-CfNPs Characterization

The physicochemical properties of *Sp*-CNPs and *Sp*-CfNPs were compared to κ-carrageenan, Cf, and *Sp* extract. The aim is to see the difference in physicochemical properties before and after the material's nanoencapsulation process, as shown in Table 2. PDI and particle sizes are the main physicochemical properties that affect the endocytosis-dependent cellular uptake.[43] PDI describes the uniformity of particle size distribution, which is calculated from two parameters, according to the correlation data (cumulance analysis). The PDI of κ-carrageenan, and Cf is 0.82 ± 0.02, and 1.00 ± 0.00, respectively. The numbers indicate that both polymers have a very broad particle size distribution with PDI > 0.7. [44] *Sp*-CNPs, and *Sp*-CfNPs had 0.65 ± 0.03, and 0.57 ± 0.02 PDI, respectively, which shows that the two nanocapsules have a fairly uniform particle size. This was inferred from the PDI value of <0.7, and shows that the distribution of the algorithm operates well.

There are many variations in the size of nanoparticles, but most have sizes between 100-500 nm.[45] The smaller the size of the nanoparticles, this causes the greater ratio of surface area to volume. This will cause more drugs to be closer to the surface of smaller particles compared to larger molecules. Drug release will be faster when it is near or attached to the surface.[46] *Sp*-CNPs and *Sp*-CfNPs showed a satisfactory particle size, 93.15 ± 3.58, and 79.59 ± 10.31 nm, respectively. This shows that the nanoencapsulation of *Sp* extract with κ-carrageenan, and Cf can yield good results with a particle size <100 nm.

Zeta potential (ζ) data (Table 2) successfully validated the capsulation extract of κ-carrageenan and folate carrageenan. The data showed κ-carrageenan has a low ζ value (about -14.10 mV) due to massive hydroxyl groups (-OH) expressing the polymer. The existence of chemical modification by folic acid on κ-carrageenan increased the zeta value up -5.29 ± 0.66 mV. This condition was mostly caused by an amine group (-NH_2) from folic acid that actively involved increasing the value of ζ of Cf. The encapsulation process of *Sp* extract with κ-carrageenan (*Sp*-CNPs) decreased the value of ζ to -8.34 ± 0.34 mV due to the strong -OH side. The interesting phenomenon happened to *Sp*-CfNPs. Supposedly, the presence of the -NH_2 group on Cf as a matrix on *Sp*-CfNPs increases the value of ξ, but this does not happen. This is possible because the electropositive side of Cf is blocked by the massive electronegative side of *Sp* extract and Cf itself. This statement is supported by the smaller particle size of *Sp*-CfNPs compared to the particle size of κ-carrageenan, Cf, *Sp* extract, and *Sp*-CNPs. Increasing the particle's size opens up more significant opportunities for obstruction of the electropositive side by the electronegative side of κ-carragenan, *Sp* extract, and folic acid in Cf. Relying on the surface charge of the *Sp*-CfNPs returned by the electronegative side, so the value rises (-12.07 ± 0.29 mV).

The characteristic FTIR absorptions of *Sp*-CNPs showed the combination of the peak of κ-carrageenan and *Sp* extract. This can be seen as absorption at 1742 cm^{-1}, a characteristic of carbonyl groups from *Sp* metabolite, whereas absorption at 1597 and 1402 cm^{-1} are polymer bound water and sulfate stretching of κ-carrageenan, respectively (Figure 6A). According to Fig. 6B, *Sp*-CfNPs shows a peak at wave number 1729 (C = O), and 1640 (C-C in ring) cm^{-1}, which is part of the *Sp* extract. The peak at 1586 cm^{-1}, which coincides with the C-C peak ring in the *Sp* extract, is the polymer bound water from κ-carrageenan, while the peak at 1408 cm^{-1} is the sulfate stretching.

The characterization of nanocapsules with TGA shows that decomposition of *Sp*-CNPs at 202^{o}C and 298^{o}C were characteristic of the κ-carrageenan matrix decomposition (Figure 7A). At *Sp*-CfNPs decomposition at 198 ^oC and 300 ^oC, it indicates the decomposition of the Cf matrix (Figure 7B) (Supplementary Fig S7). The absence of decomposition of the two nanocapsules at a temperature of 400 – 600 ^oC which is a characteristic of the of the *Sp* extract decomposition, is caused by the amount of κ-carrageenan and Cf degradation. While the

ISSN 2616-0684 (Print)
ISSN 2616-0692 (Electronic)

Sp extract concentration is very low, this is supported by a small loading amount of data.
The morphology of *Sp*-CNPs and *Sp*-CfNPs was found to be spherical. Some particles have sizes above 100 nm, but most *Sp*-CNPs and *Sp*-CfNPs particles were less than 100 nm **(**Figure 8**)**.

Sp-CNPs and Sp-CfNPs Stability

The stability of both nanocapsules was influenced by the nature of the matrix used, κ-carrageenan and carrageenan folate. *Sp*-CNPs turbidity decreased at 30 ^{o}C – 80 ^{o}C and has an increase in turbidity at 90 ^{o}C – 100 ^{o}C. It was suspected that the κ-carrageenan matrix formed a gel caused by depolymerization. Both nanocapsules (*Sp*-CNPs and *Sp*-CfNPs) tend to be stable at basic pH. This can be seen from the low turbidity level. While the pH of turbidity increases. κ-carrageenan is susceptible to depolymerization through acid-catalyzed hydrolysis. [47] κ-carrageenan is not hydrolyzed at pH 8 and the molecular mass is relatively fixed at > 200 kDa, with no more than 20% has a molecular mass of < 100 kDa.[48] Increasing of NaCl concentrations cause increased turbidity in both nanocapsules. The increasing turbidity of the two nanocapsules is presumably because the matrix of the nanocapsules is gelated with Na^{+} ions, which results in aggregation of particles from the two nanocapsules. The second bioactive component of nanocapsules is relatively stable at changes in temperature and salt addition, but is not stable at in pH changes. (Supplementary Fig S8 – S11).

Loading and release

The loading efficiency is expressed as the percentage of Sp that was successfully trapped in micelles or encapsulated. The percentage value of LE *Sp*-CNPs and *Sp*-CfNPs 73.32% (9,165 mg) and 81.82% (10.227 mg). Whereas, the amount of loading can be calculated by the number of trapped *Sp* divided by the total of NPs. The percentage value of LA *Sp*-CNPs and *Sp*-CfNPs is 14.66% (1.833 mg) and 16.36% (2.045 mg).
Particle size and particle size distribution have important roles in nanoparticulate systems such as drug loading capacity, drug release and nanoparticle system stability. Smaller particles have a wider area, this causes faster drug release, while larger particles have a large core surface, the spread occurs gradually.[49] The percentage release of bioactive compound (3,4,3'-tri-*O*-methyl ellagic acid) from *Sp*-CNPs, and *Sp*-CfNPs is shown in Figure 9. The release of active components from *Sp*-CNPs and *Sp*-CfNPs was detected using a UV-Vis spectrometer. Absorbance measurements were carried out at a wavelength of 372 nm, which is the maximum wavelength of 3,4,3'-tri-O-methyl ellagic acid. The release test was carried out for 24 h. The best release for both *Sp*-CNPs, and *Sp*-CfNPs after 24 h was at pH 9, whereas the percentage of release was 45.13% and 60.41%, respectively.
Meanwhile, the release at pH 4 for both was the lowest, *i.e.*, 37.41% and 51.04%, respectively. In general, *Sp*-CfNPs showed better releases than *Sp*-CNPs at all pH values. Poor release of acidic pH was possibly due to the aggregation caused by a decrease in the particle's electrostatic repulsion. The κ-carrageenan and carrageenan folate sites in *Sp*-CNPs and *Sp*-CfNPs are electronegative. In alkaline conditions, both of nanocapsules repulsion occurs between particles, causing enlargement of nanocapsule particle's pores, facilitating of bioactive components release. Conversely, in acidic conditions, there is a pull between particles caused by hydrogen bonds formed, so that the pores of the particles are small and release slightly (Figure 9).

Anticancer Activity Evaluation

The difference between *Sp*-CNPs and *Sp*-CfNPs is the presence or absence of folic acid as a selective target of folate receptors on cancer cells. Cancer cells have an expression of folate receptors. Alpha receptor folate (FRα) can be found in cervical and breast cancer cells.[50] Targeting folate-based receptor drugs is based on the attachment of folate-drug conjugate ligands into the cytosol of cells with endocytosis.[51]

The results on both cancer cells (HeLa and T47D) showed that the nanoencapsulation process of *Sp* with the main component 3,4,3'- tri-O-methyl ellagic acid has been able to increase the anticancer activity that can be observed from the cell viability of both cancer cells (Figure 10).

Table 1: Correlation of ^{1}H and ^{13}C- NMR chemical shift values

Position	Isolate Compound		Reference[39]	
	δ_C	δ_H	δ_C	δ_H
1	112.0 (C)		111.6 (C)	
2	141.5 (C)		141.2 (C)	
3	140.9 (C)		140.3 (C)	
4	152.8 (C)		152.2 (C)	
5	107.5 (CH)	7.63 (s)	111.4 (CH)	7.73 (s)
6	112.6 (C)		112.1 (C)	
7	158.6 (C=O)		158.5 (C=O)	
1'	111.1 (C)		111.7 (C)	
2'	141.0 (C)		141.3 (C)	
3'	140.3 (C)		140.2 (C)	
4'	153.8 (C)		152.2 (C)	
5'	1117 (CH)	7.52 (s)	111.5 (CH)	7.61 (s)
6'	112.0 (C)		112.1 (C)	
7'	158.4 (C=O)		158.6 (C=O)	
3-OCH_3	61.3 (CH_3)	4.03 (s)	61.5 (CH_3)	4.19 (s)
4-OCH_3	56.7 (CH_3)	3.99 (s)	56.5 (CH_3)	4.04 (s)
3'-OCH_3	61.0 (CH_3)	4.04 (s)	61.3 (CH_3)	4.14 (s)

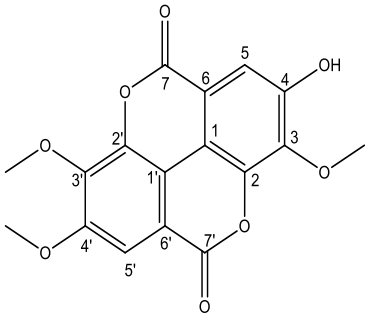

Figure 1: Structure of 3,4,3'-tri-*O*-methyl ellagic acid

Table 2: Physicochemical properties of Sp-CNPs and Sp-CfNPs

Type	PDI ± SD	Size ± SD (nm)	ζ ± SD (mV)
κ-Carrageenan	0.82 ± 0.02	870.48 ± 26.94	-14.10 ±0.00
Cf	1.00 ± 0.00	926.50 ± 5.52	-5.29 ± 0.66
Sp Extract	0.59 ± 0.03	226.35 ± 5.58	-3.30 ± 0.58
Sp-CNPs	0.65 ± 0.03	93.15 ± 3.58	-8.34 ± 0.34
Sp-CfNPs	0.57 ± 0.02	79.59 ± 10.31	-12.07 ±0.29

Each data presented as mean ± SD (n=3)

ISSN 2616-0684 (Print)
ISSN 2616-0692 (Electronic)

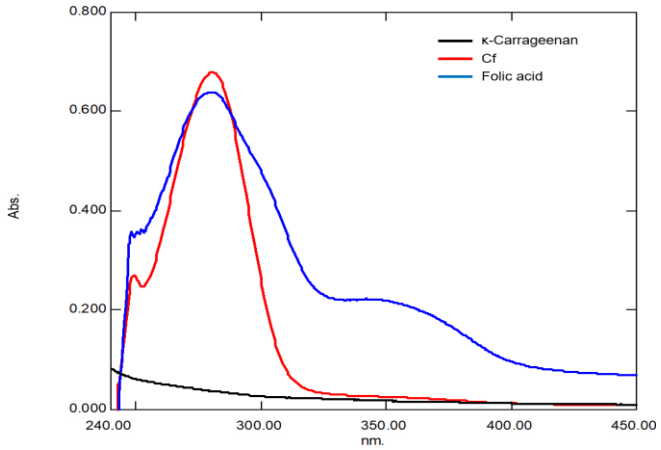

Figure 2: UV-Vis spectrum of κ-carrageenan Cf and folic acid

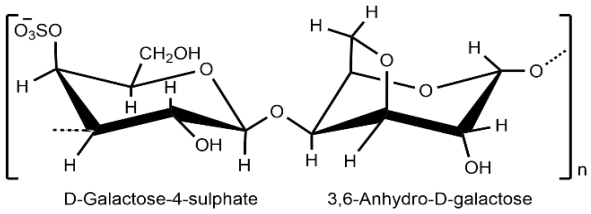

Figure 3: Structure of κ- carrageenan

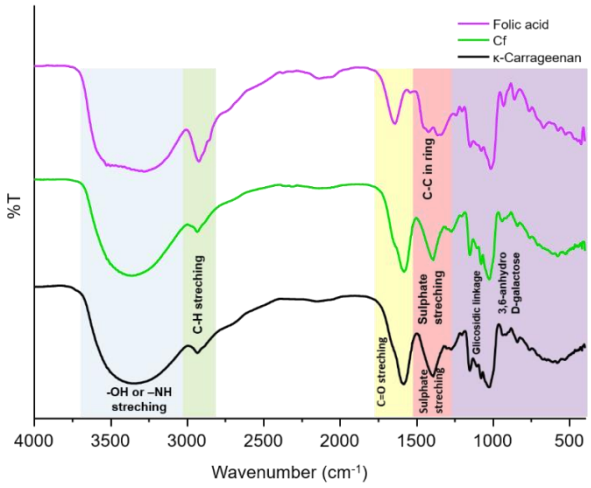

Figure 4: FTIR spectrum of κ-carrageenan, Cf, and folic acid

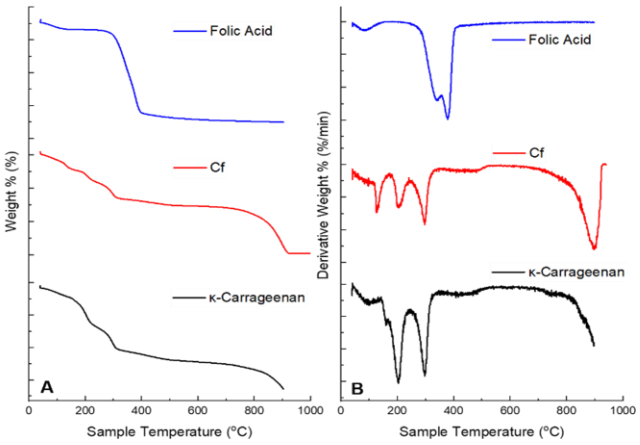

Figure 5: Thermogram data of κ-carrageenan, Cf, and folic acid. **A)** Beginning, and **B)** Derived functions

Free *Sp* is able to inhibit the growth of HeLa cancer cells with EC_{50} ± SE 114.19 ± 10.31 µg / mL. After encapsulation using κ-carrageenan (*Sp*-CNPs), the inhibitory activity of HeLa cancer cell growth increased to EC_{50} ± SE 79.19 ± 13.96 µg / mL. Similarly, when *Sp* extract was encapsulated with carrageenan folate (*Sp*-CfNPs) the inhibitory activity of HeLa cells became EC_{50} ± SE 48.77 ± 15.91 µg / mL. As for the single acid compound 3,4,3 '-tri-O-methyl ellagic acid has an EC_{50} ± SE value of 12.58 ± 2.23 µg / mL.

Anticancer activity of free *Sp* in T47D cells showed EC_{50} ± SE values 498.33 ± 110.72 µg / mL. *Sp*-CNPs nanocapsules have increased the anticancer activity of *Sp* extract with EC_{50} ± SE 80.62 ± 12.59 µg / mL. Whereas *Sp*-CfNPs have anticancer activity against T47D cells with EC_{50} ± SE 48.52 ± 2.76 µg / mL. The single acid compound 3,4,3'-tri-O-methyl ellagic acid in T47D cells showed an EC_{50} ± SE value of 55.64 ± 6.29 µg / mL. FR in ovarian / cervical cancer is 90% while in breast cell is 48%.[52] Free *Sp* on the HeLa cell line had better inhibitory activity than on the T47D cell line. Based on the ANOVA analysis, it was found that the nanoencapsulation process of *Sp* extract with κ-carrageenan and carrageenan folate on the HeLa cell line did not have a significant effect on the cell inhibitory activity, with a value of p = 0.289 for *Sp*-CNPs and p = 0.802 for *Sp*-CfNPs. Whereas the T47D cell line shows the inhibitory activity of these cells had significantly by both nanocapsules. *Sp*-CfNPs on T47D cell lines have a value of p = 0.008, while *Sp*-CNPs have a value of p = 0.042. This shows that the folate group's T47D cells in nanocapsules show better activity than κ-carrageenan use.

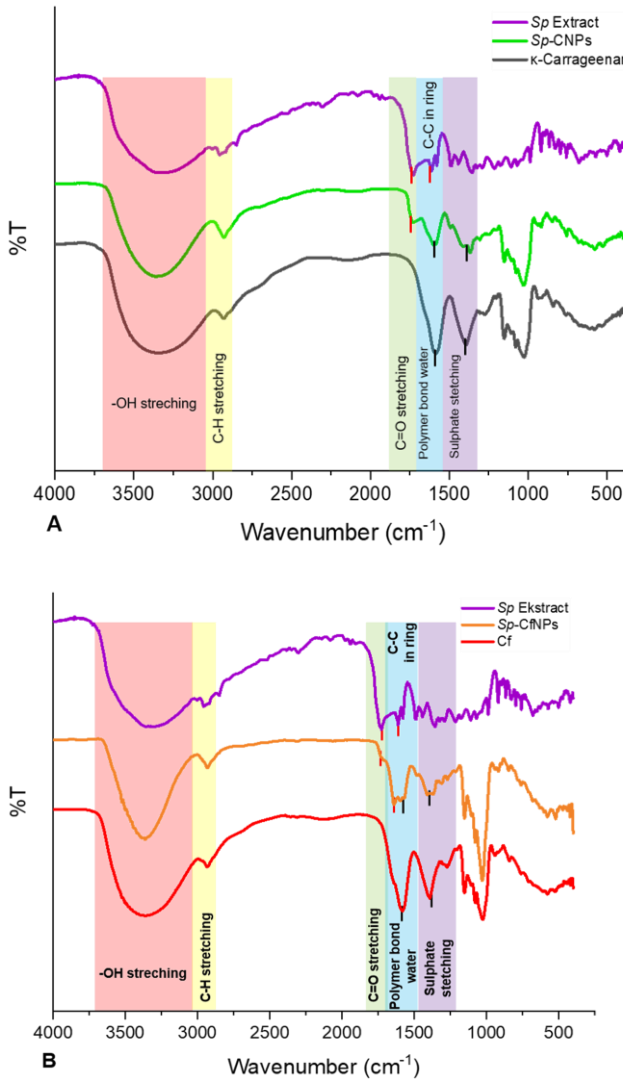

Figure 6: Spectrum of FTIR **A)** *Sp*-CNPs dan **B)** *Sp*-CfNPs

ISSN 2616-0684 (Print)
ISSN 2616-0692 (Electronic)

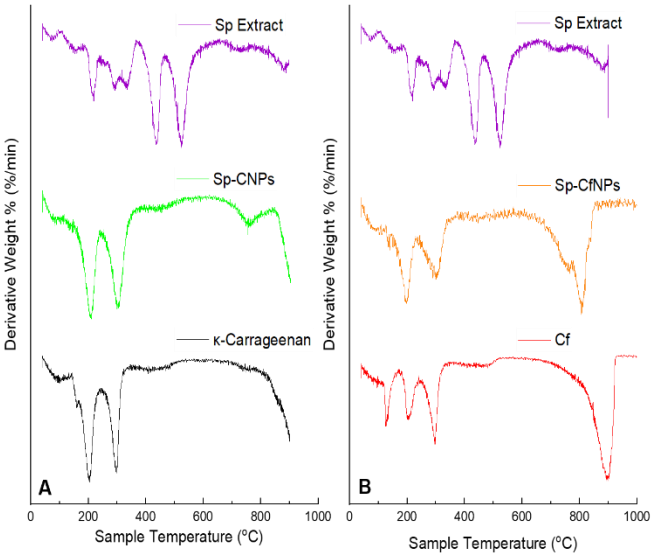

Figure 7: Thermograms **A)** Derivative *Sp*-CNPs, and **B)** Derivative *Sp*-CfNPs

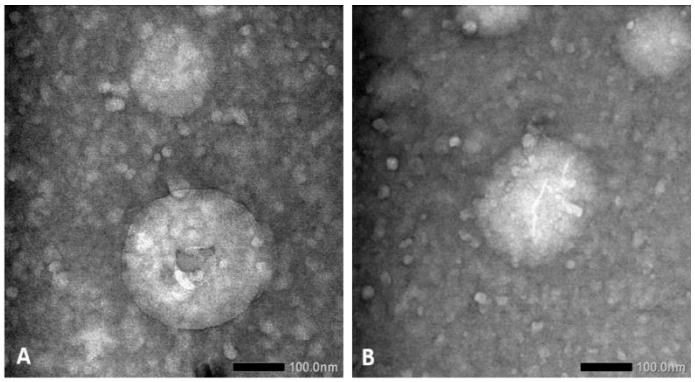

Figure 8: TEM Images of **A)** *Sp*-CNPs dan **B)** *Sp*-CfNPs scale bar refer to 100 nm

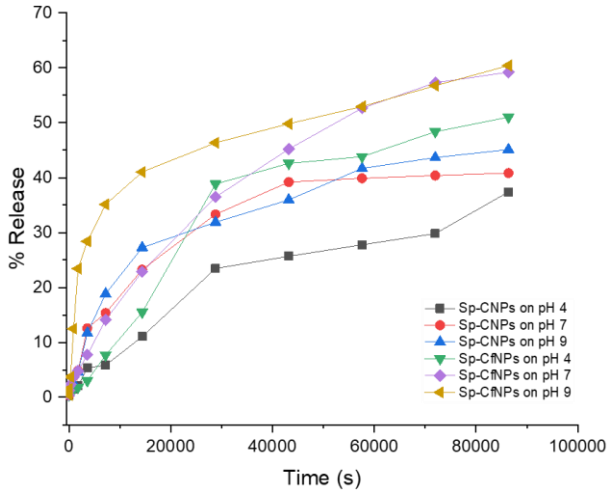

Figure 9: The release of the Sp extract bioactive components from *Sp*-CNPs and *Sp*-CfNPs

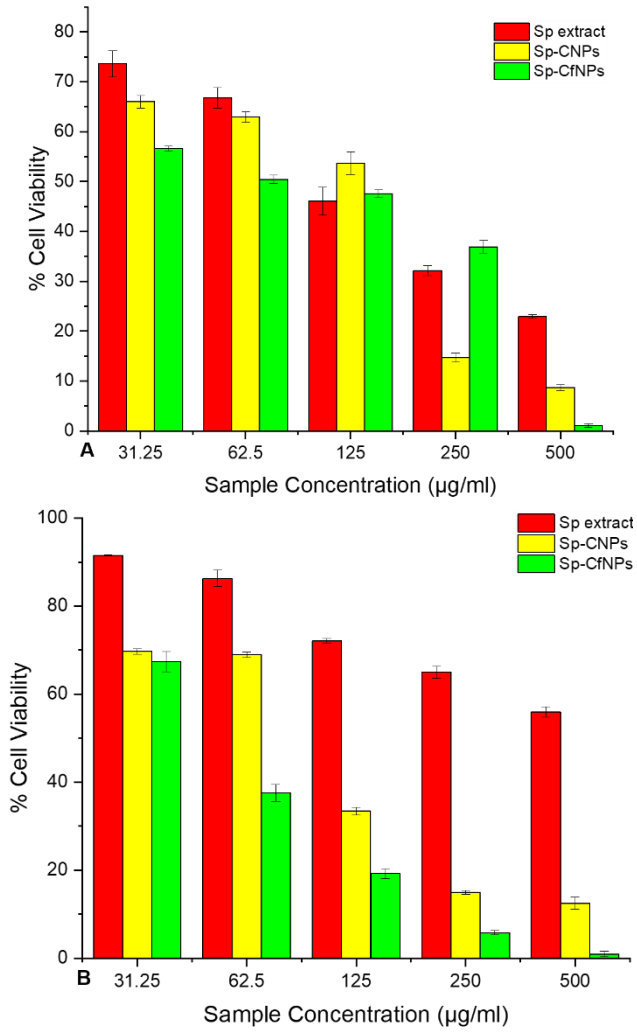

Figure 10: Cell viability with MTT assay **A)** HeLa cells, and **B)** T47D cells

Conclusion

3,4,3'-Tri-*O*-methyl ellagic acid in the *S. polycephalum* extract, derivative of ellagic acid, showed a good *in-vitro* anticancer activity against HeLa cell line and T47D cell line. Development of κ-carrageenan, and carrageenan folate as a drug delivery system to increase the bioactivity of the *Sp* extract. *Sp*-CfNPs increase the inhibitory activity of HeLa cell lines and T47D cell lines than *Sp*-CNPs. However, only the T47D cell line showed a significant increase in the *Sp* extract activity, while it did not work/come in the HeLa cell line. This promising result shows that the presence of folate ions in *Sp* extract nanocapsules increases the inhibitory activity of cancer cells *in-vitro* by targeting folate receptors.

Conflict of interest

The authors declare no conflict of interest.

Authors' Declaration

The authors hereby declare that the work presented in this article is original and that any liability for claims relating to the content of this article will be borne by them.

Acknowledgments

The authors would like to express gratitude to: The Ministry of Research and Technology, Republic of Indonesia, for support through the 2020 Flagship University Research: "PENELITIAN DASAR UNGGULAN PERGURUAN TINGGI (PDUPT)" Research Scheme with contract number: 817/UN3.14/PT/2020, Faculty of Pharmacy, Meijo University, Nagoya, Japan for DART-MS, and H. E. J. Research Institute of Chemistry, International Center for Chemical and Biological Sciences, University of Karachi, Karachi-75270, Pakistan for 1D and 2D NMR data.

References

1. Torre LA, Bray F, Siegel RL, FerlayJ, Lortet-Tieulent J, Jemal A. Global cancer statistics, 2012. CA Cancer J Clin. 2015; 65(2):87-108.
2. Bray F, Ferlay J, Soerjomataram I, Siegel RL, Torre LA, JemalA. Global cancer statistics 2018: GLOBOCAN estimates of incidence and mortality worldwide for 36 cancers in 185 countries. CA Cancer J Clin. 2018; 68(6): 394-424.
3. Nussbaumer S, Bonnabry P, Veuthey JL, Fleury-Souverain S. Analysis of anticancer drugs: a review. Talanta. 2011; 85(5):2265-2289.
4. Hosseini A and Ghorbani A. Cancer therapy with phytochemicals: evidence from clinical studies. Avicenna J Phytomed. 2015; 5(2):84-97.
5. Greenwell M and Rahman P. Medicinal plants: their use in anticancer treatment. Int J Pharm Sci Res. 2015; 6(10): 4103-4112.
6. Cheung A, Bax HJ, Josephs DH, Ilieva KM, Pellizzari G, Opzoomer J, Bloomfield J, Fittall M, Grigoriadis A, Figini M. Targeting folate receptor alpha for cancer treatment. Oncotarget. 2016; 7(32):52553.
7. Zwicke GL, Ali Mansoori G, Jeffery CJ. Utilizing the folate receptor for active targeting of cancer nanotherapeutics. Nano Reviews. 2012; 3(1):18496.
8. Gupta A, Kaur CD, Saraf S. Targeting of herbal bioactives through folate receptors: a novel concept to enhance intracellular drug delivery in cancer therapy. J Recept Signal Transduct. 2017; 37(3):314-323.
9. Ledermann J, Canevari S, Thigpen T. Targeting the folate receptor: diagnostic and therapeutic approaches to personalize cancer treatments. Ann Oncol. 2015; 26(10):2034-2043.
10. Müller C and Schibli R .Folic acid conjugates for nuclear imaging of folate receptor–positive cancer. J Nucl Med. 2011; 52(1):1-4.
11. Khodavirdipour A, Zarean R, Safaralizadeh R. Evaluation of the Anti-cancer Effect of *Syzygium cumini* Ethanolic Extract on HT-29 Colorectal Cell Line. J Gastrointes Cancer 2020.
12. Kubatka P, Uramova S, Kello M, Kajo K, Kruzliak P, Mojzis J, Vybohova D, Adamkov M, Jasek K, Lasabova Z. Antineoplastic effects of clove buds (*Syzygium aromaticum* L.) in the model of breast carcinoma. J Cell Mol Med. 2017; 21(11): 2837-2851.
13. Memon AH, Ismail Z, Aisha AF, Al-Suede FSR, Hamil MSR, Hashim S, Saeed MAA, Laghari M, Majid A, Shah AM. Isolation, characterization, crystal structure elucidation, and anticancer study of dimethyl cardamonin, isolated from *Syzygium campanulatum* Korth. Evid Based Complement Alternat Med. 2014; 2014:1-11.
14. Thampi N and Shalini JV. Bio-prospecting the in-vitro antioxidant and anti-cancer activities of silver nanoparticles synthesized from the leaves of *Syzygium samarangense*. Int J Pharm Pharm Sci. 2015; 7(7):269-274.
15. Annadurai G, Masilla BRP, Jothiramshekar S, Palanisami E, Puthiyapurayil S, Parida AK. Antimicrobial, antioxidant, anticancer activities of *Syzygium caryophyllatum* (L.) Alston. Int J Green Pharm. 2012; 6(4):285-288.
16. Kiruthiga K, Saranya J, Eganathan P, Sujanapal P, Parida A. Chemical composition, antimicrobial, antioxidant and anticancer activity of leaves of *Syzygium benthamianum* (Wight ex Duthie) Gamble. JBAPN. 2011; 1(4):273-278.
17. Islam S, Nasrin S, Khan MA, Hossain AS, Islam F, Khandokhar P, Mollah MNH, Rashid M, Sadik G, Rahman MAA. Evaluation of antioxidant and anticancer properties of the seed extracts of *Syzygium fruticosum* Roxb. growing in Rajshahi, Bangladesh. BMC Compl Altern Med. 2013; 13(142):1-10.
18. Komuraiah B, Chinde S, Kumar AN, Srinivas K, Venu C, Kumar JK, Sastry K, Grover P. Isolation of phytochemicals from anticancer active extracts of *Syzygium alternifolium* Walp. leaf. Pharmacogn J. 2014; 6(4):83-85.
19. Tukiran T, Wardana AP, Hidayati N, Shimizu K. An Ellagic Acid Derivative and Its Antioxidant Activity of Stem Bark Extracts of *Syzygium polycephalum* Miq.(Myrtaceae). Indones J Chem. 2018; 18(1):26-34.
20. Wang N, Wang Q, Tang H, Zhang F, Zheng Y, Wang S, Zhang J, Wang Z, Xie X. Direct inhibition of ACTN4 by ellagic acid limits breast cancer metastasis via regulation of *β*-catenin stabilization in cancer stem cells. J Exp Clin Cancer Res. 2017; 36(1):172.
21. Xu W, Xu J, Wang T, Liu W, Wei H, Yang X, Yan W, Zhou W, Xiao J. Ellagic acid and Sennoside B inhibit osteosarcoma cell migration, invasion and growth by repressing the expression of c-Jun. Oncol Lett. 2018; 16 (1):898-904.
22. Cheng H Lu C, Tang R, Pan Y, Bao S, Qiu Y, Xie M. Ellagic acid inhibits the proliferation of human pancreatic carcinoma PANC-1 cells *in vitro* and *in vivo*. Oncotarget 2017; 8(7):12301.
23. Liu H, Zeng Z, Wang S, Li T, Mastriani E, Li QH, Bao HX, Zhou YJ, Wang X, Liu Y. Main components of pomegranate, ellagic acid and luteolin, inhibit metastasis of ovarian cancer by down-regulating MMP2 and MMP9. Cancer Biol Ther. 2017; 18(12):990-999.
24. Huang ST, Wang CY, Yang RC, Chu CJ, Wu HT, Pang JH S. *Phyllanthus urinaria* increases apoptosis and reduces telomerase activity in human nasopharyngeal carcinoma cells. Complement Med Res. 2009; 16(1):34-40.
25. Mishra S and Vinayak M. Ellagic acid inhibits PKC signaling by improving antioxidant defense system in murine T cell lymphoma. Mol Biol Rep. 2014; 41(7):4187-4197.
26. Eskandari E, Heidarian E, Amini S, Saffari-Chaleshtori J. Evaluating the effects of ellagic acid on pSTAT3, pAKT, and pERK1/2 signaling pathways in prostate cancer PC3 cells. J Cancer Res Ther. 2016; 12(4):1266-1271.
27. Mirsane S. Benefits of ellagic acid from grapes and pomegranates against colorectal cancer. Caspian J Intern Med. 2017; 8(3):226-227.
28. Bisen P, Bundela S, Sharma A. Ellagic acid-chemopreventive role in oral cancer. J Cancer Sci Ther. 2012; 4(2):23-30.
29. Zhang H, Guo ZJ, Xu WM, You ZJ, Han L, Han YX, Dai LJ. Antitumor effect and mechanism of an ellagic acid derivative on the HepG2 human hepatocellular carcinoma cell line. Oncol Lett. 2014; 7(2):525-530.
30. de Molina AR, Vargas T, Molina S, Sánchez J, Martínez-Romero J, González-Vallinas M, Martín-Hernández R, Sánchez-Martínez R, de Cedrón MG, Dávalos A. The ellagic acid derivative 4, 4′-di-O-methylellagic acid efficiently inhibits colon cancer cell growth through a mechanism involving WNT16. J Pharmacol Exp Ther. 2015; 353(2):433-444.
31. Alfei S, Turrini F, Catena S, Zunin P, Parodi B, Zuccari G, Pittaluga AM, Boggia R. Preparation of ellagic acid micro and nano formulations with amazingly increased water

solubility by its entrapment in pectin or non-PAMAM dendrimers suitable for clinical applications. New J Chem. 2019; 43(6):2438-2448.
32. Neamatallah T, El-Shitany N, Abbas A, Eid BG, Harakeh S, Ali S, Mousa S. Nano Ellagic Acid Counteracts Cisplatin-Induced Upregulation in OAT1 and OAT3: A Possible Nephroprotection Mechanism. Molecules. 2020; 25(13):3031
33. El-Shitany NA, Abbas AT, Ali SS, Eid B, Harakeh S, Neamatallah T, Al-Abd A, Mousa S. Nanoparticles Ellagic Acid Protects Against Cisplatin-induced Hepatotoxicity in Rats Without Inhibiting its Cytotoxic Activity. Int J Pharmacol. 2019; 15(4):465-477.
34. Badawi NM, Teaima MH, El-Say KM, Attia DA, El-Nabarawi MA, Elmazar MM. Pomegranate extract-loaded solid lipid nanoparticles: design, optimization, and *in vitro* cytotoxicity study. Int J Nanomedicine. 2018; 13:1313.
35. Yao H, Liu J, Xu S, Zhu Z, Xu J. The structural modification of natural products for novel drug discovery. Expert Opin Drug Discov. 2017; 12(2):121-140.
36. Bharali DJ and Mousa SA. Emerging nanomedicines for early cancer detection and improved treatment: current perspective and future promise. Pharmacol Ther. 2010; 128(2):324-335.
37. Mehrnia MA, Jafari SM, Makhmal-Zadeh BS, Maghsoudlou Y. Crocin loaded nano-emulsions: factors affecting emulsion properties in spontaneous emulsification. Int J Biol Macromol. 2016; 84:261-267.
38. Fahmi MZ, Haris A, Permana AJ, Wibowo DLN, Purwanto B, Nikmah YL, Idris A. Bamboo leaf-based carbon dots for efficient tumor imaging and therapy. RSC Adv. 2018; 8(67): 38376-38383.
39. Gao X, Wu J, Zou W, Dai Y. Two ellagic acids isolated from roots of Sanguisorba officinalis L. promote hematopoietic progenitor cell proliferation and megakaryocyte differentiation. Molecules 2014; 19(4):5448-5458.
40. Tsakos M, Schaffert ES, Clement LL, Villadsen NL, Poulsen TB. Ester coupling reactions–an enduring challenge in the chemical synthesis of bioactive natural products. Nat Prod Rep. 2015; 32(4):605-632.
41. Mangione M, Giacomazza D, Bulone D, Martorana V, San Biagio P. Thermoreversible gelation of κ-Carrageenan: relation between conformational transition and aggregation. Biophysl Chem. 2003; 104(1):95-105.
42. Towle GA. Carrageenan. In Industrial gums, Elsevier: 1973; pp 83-114.
43. Danaei M, Dehghankhold M, Ataei S, Hasanzadeh Davarani F, Javanmard R, Dokhani A, Khorasani S, Mozafari M. Impact of particle size and polydispersity index on the clinical applications of lipidic nanocarrier systems. Pharmaceutics 2018; 10(2):1-17.
44. Worldwide MI. Dynamic light scattering, Common terms defined. Inform white paper. Malwern Instruments Limited. 2011; 2011:1-6.
45. Rizvi SA, Saleh AM. Applications of nanoparticle systems in drug delivery technology. Saudi Pharmaceutical Journal 2018; 26(1):64-70.
46. Buzea C, Pacheco II, Robbie K. Nanomaterials and nanoparticles: sources and toxicity. Biointerphases. 2007; 2 (4):MR17-MR71.
47. Stanley N. Production, properties and uses of carrageenan. Production and utilization of products from commercial seaweeds. FAO Fisheries Technical Paper. 1987; 288:116-146.
48. Capron I, Yvon M, Muller G. In-vitro gastric stability of carrageenan. Food hydrocolloids. 1996; 10(2):239-244.
49. Redhead H, Davis S, Illum L. Drug delivery in poly (lactide-co-glycolide) nanoparticles surface modified with poloxamer 407 and poloxamine 908: *in vitro* characterisation and *in vivo* evaluation. J Control Release. 2001; 70(3):353-363.
50. Parker N, Turk MJ, Westrick E, Lewis JD, Low PS, Leamon CP. Folate receptor expression in carcinomas and normal tissues determined by a quantitative radioligand binding assay. Anal Biochem. 2005; 338(2):284-293.
51. Fernández M, Javaid F, Chudasama V. Advances in targeting the folate receptor in the treatment/imaging of cancers. Chem Sci. 2018; 9(4):790-810.
52. Low PS and Kularatne SA. Folate-targeted therapeutic and imaging agents for cancer. Curr Opin Chem Biol. 2009; 13 (3):256-262.